Supplementary Information

Evaluation of reduction efficiencies of pepper mild mottle virus and human enteric viruses in full-scale drinking water treatment plants employing coagulation-sedimentation–rapid sand filtration or coagulation–microfiltration

D. Shirakawa, N. Shirasaki*, T. Matsushita, Y. Matsui, R. Yamashita, T. Matsumura, S. Koriki

Division of Environmental Engineering, Faculty of Engineering, Hokkaido University, N13W8, Sapporo 060-8628, Japan

* Corresponding author. Tel.: +81-11-706-7282; fax: +81-11-706-7282.

E-mail address: nobutaka@eng.hokudai.ac.jp (N. Shirasaki)

Table S1

Sequences of primers and probes used in the present study.

Viruses		Oligonucleotide sequences (5'->3')[a]	Positions[b]	References
Pepper mild mottle virus	Forward primer	GAG TGG TTT GAC CTT AAC GTT TGA	1878–1901	Haramoto *et al*., 2013
	Reverse primer	TTG TCG GTT GCA ATG CAA GT	1945–1926	
	TaqMan probe	FAM-CCT ACC GAA GCA AAT G-TAMRA	1906–1921	Zhang *et al*., 2006
	TaqMan MGB probe	FAM-CCT ACC GAA GCA AAT G-MGB-NFQ	1906–1921	
Cucumber green mottle virus	Forward primer	GCA TAG TGC TTT CCC GTT CAC	6285–6305	
	Reverse primer	TGC AGA ATT ACT GCC CAT AGA AAC	6385–6362	Hongyun *et al*., 2008
	TaqMan probe	FAM-CGG TTT GCT CAT TGG TTT GCG GA-TAMRA	6316–6338	
Adenovirus	Forward primer	AAC TTT CTC TCT TAA TAG ACG CC	30372–30394	
	Reverse primer	AGG GGG CTA GAA AAC AAA A	30489–30471	Ko *et al*., 2005
	TaqMan probe	FAM-CTG ACA CGG GCA CTC TTC GC-TAMRA	30405–30424	
Enteroviruses including coxsackievirus	Forward primer	CCT CCG GCC CCT GAA TG	449–465	Shieh *et al*., 1995
	Reverse primer	ACC GGA TGG CCA ATC CAA	643–626	
	TaqMan probe	FAM-CCG ACT ACT TTG GGT GTC CGT GTT TC-TAMRA	542–567	Katayama *et al*., 2002
Hepatitis A virus	Forward primer	GGT AGG CTA CGG GTG AAA C	393–411	
	Reverse primer	AAC AAC TCA CCA ATA TCC GC	481–462	Jothikumar *et al*., 2005
	TaqMan probe	FAM-CTT AGG CTA ATA CTT CTA TGA AGA GAT GC-TAMRA	414–442	

Table S1 (*continued*)

Viruses		Oligonucleotide sequences (5'->3')[a]	Positions[b]	References
Human norovirus GI	Forward primer	CGY TGG ATG CGI TTY CAT GA	5291–5310	Vega *et al*., 2011
	Reverse primer	CTT AGA CGC CAT CAT CAT TYA C	5375–5354	
	TaqMan probe	FAM-AGA TYG CGI TCI CCT GTC CA-TAMRA	5340–5321	
Human norovirus GII	Forward primer	CAR GAR BCN ATG TTY AGR TGG ATG AG	5003–5028	Vega *et al*., 2011
	Reverse primer	TCG ACG CCA TCT TCA TTC ACA	5100–5080	
	TaqMan probe	FAM-TGG GAG GGC GAT CGC AAT CT-TAMRA	5048–5067	
Murine norovirus	Forward primer	CCG CAG GAA CGC TCA GCA G	5028–5046	Kitajima *et al*., 2010
	Reverse primer	GGY TGA ATG GGG ACG GCC TG	5156–5137	
	TaqMan probe	FAM-ATG AGT GAT GGC GCA-TAMRA	5062–5076	
	TaqMan MGB probe	FAM-ATG AGT GAT GGC GCA-MGB-NFQ	5062–5076	
MS2	Forward primer	GTC GCG GTA ATT GGC GC	632–648	O'Connell *et al*., 2006
	Reverse primer	GGC CAC GTG TTT TGA TCG A	708–690	
	TaqMan probe	FAM-AGG CGC TCC GCT ACC TTG CCC T-TAMRA	650–671	

[a] FAM, 6-carboxyfluorescein; TAMRA, 6-carboxytetramethylrhodamine; MGB, minor groove binder; NFQ; nonfluorescent quencher.

[b] Genebank accession numbers for sequence positions are AB254821 for pepper mild mottle virus, D12505 for cucumber green mottle mosaic virus, NC_001454 for adenovirus, AF114383 for enteroviruses including coxsackievirus, M14707 for hepatitis A virus, M87661 for human norovirus GI, U07611 for human norovirus GII, NC_008311 for murine norovirus, and NC_001417 for MS2.

Table S2

Water quality data for raw and treated water samples collected at Plants A–D.

		Water type	Temperature (°C)	pH	Turbidity (NTU)	DOC (mg/L)	UV260 (cm^{-1})	Alkalinity (mg-$CaCO_3$/L)	Coagulant dosage (mg-Al/L)
Plant A	Oct. 2017	Raw water	10.5	7.4	1.4	0.8	0.024	18.2	1.7
		After CS	ND[a]	7.1	0.2	0.5	0.010	15.0	
		After RSF	ND	7.1	0.13	0.5	0.007	15.6	
	Nov. 2017	Raw water	7.7	7.3	2.4	1.2	0.036	18.4	1.3
		After CS	ND	7.3	0.3	0.7	0.013	17.6	
		After RSF	ND	7.4	0.10	0.7	0.010	17.0	
	Dec. 2017	Raw water	3.3	7.3	1.2	0.9	0.026	17.0	1.6
		After CS	ND	7.3	0.3	0.6	0.011	16.4	
		After RSF	ND	7.2	0.11	0.5	0.008	16.0	
	May 2018	Raw water	6.3	6.7	10.2	0.5	0.031	8.6	1.9
		After CS	ND	6.7	0.7	0.3	0.006	8.6	
		After RSF	ND	6.7	0.13	0.3	0.004	8.4	
	Jul. 2018	Raw water	13.4	7.0	4.2	0.9	0.040	13.4	1.2
		After CS	ND	6.9	0.4	0.5	0.012	12.2	
		After RSF	ND	6.8	0.12	0.6	0.008	12.2	
	Nov. 2018	Raw water	6.4	7.4	1.7	0.8	0.028	18.2	1.6
		After CS	ND	7.2	0.5	0.5	0.012	14.2	
		After RSF	ND	7.3	0.12	0.5	0.007	14.6	
	Feb. 2019	Raw water	2.5	7.3	1.4	0.7	0.022	16.6	1.5
		After CS	ND	7.1	0.4	0.4	0.009	17.4	
		After RSF	ND	7.1	0.11	0.4	0.006	16.4	
Plant B	Nov. 2017	Raw water	10.4	7.7	7.1	0.8	0.018	50.4	0.9
		After CS	ND	7.3	0.5	0.7	0.012	39.2	
		After RSF	ND	7.5	0.12	0.6	0.011	39.8	
	Aug. 2018	Raw water	26.2	7.2	9.6	1.0	0.024	49.0	1.0
		After CS	ND	6.8	0.6	0.6	0.011	33.0	
		After RSF	ND	6.9	0.13	0.6	0.011	32.8	
	Feb. 2019	Raw water	5.1	7.3	3.1	1.4	0.024	44.8	1.2
		After CS	ND	6.9	0.7	1.3	0.013	38.8	
		After RSF	ND	7.0	0.14	1.2	0.013	39.0	

Table S2 (*continued*)

		Water type	Temperature (°C)	pH	Turbidity (NTU)	DOC (mg/L)	UV260 (cm^{-1})	Alkalinity (mg-$CaCO_3$/L)	Coagulant dosage (mg-Al/L)
Plant C	May 2018	Raw water	9.7	7.0	1.7	0.5	0.013	9.4	0.3
		After pre-chlorination	ND	7.0	1.2	0.5	0.009	10.2	
		After MnOx filtration	ND	6.9	1.5	0.5	0.009	10.0	
		After C–MF	ND	7.2	0.11	0.3	0.003	11.8	
	Jul. 2018	Raw water	15.9	6.6	2.2	0.7	0.022	12.4	0.3
		After pre-chlorination	ND	6.7	2.0	0.8	0.018	12.8	
		After MnOx filtration	ND	6.8	1.6	0.8	0.016	12.6	
		After C–MF	ND	7.1	0.10	0.6	0.006	15.2	
	Nov. 2018	Raw water	8.0	6.8	1.0	0.9	0.025	12.8	0.3
		After pre-chlorination	ND	6.8	1.1	0.9	0.022	13.0	
		After MnOx filtration	ND	6.8	0.9	0.9	0.018	12.8	
		After C–MF	ND	7.2	0.10	0.6	0.008	17.2	
	Jan. 2019	Raw water	0.9	6.8	1.7	0.6	0.014	13.6	0.4
		After pre-chlorination	ND	6.9	0.7	0.6	0.012	12.8	
		After MnOx filtration	ND	6.8	0.9	0.6	0.013	14.0	
		After C–MF	ND	7.1	0.10	0.4	0.006	16.4	
	Jul. 2019	Raw water	20.0	7.1	0.6	1.1	0.027	19.0	0.3
		After pre-chlorination	ND	7.0	0.6	1.1	0.022	19.0	
		After MnOx filtration	ND	7.2	0.5	1.1	0.019	20.0	
		After C–MF	ND	7.2	0.11	0.8	0.011	24.0	
Plant D	Jul. 2020	Raw water	17.7	7.0	8.7	1.6	0.044	27.0	0.4
		After coagulation	ND	7.0	8.8	1.2	0.021	27.8	
		After MF	ND	7.7	0.08	1.2	0.019	30.0	
	Nov. 2020	Raw water	8.3	7.3	2.8	1.9	0.056	49.0	0.4
		After coagulation	ND	7.3	9.1	1.7	0.037	55.0	
		After MF	ND	7.8	0.12	1.6	0.026	57.0	
	Jan. 2021	Raw water	0.6	7.7	5.0	1.5	0.036	64.2	0.4
		After coagulation	ND	7.6	7.8	1.2	0.020	63.0	
		After MF	ND	7.8	0.08	1.2	0.017	64.6	
	Mar. 2021 (9th)	Raw water	0.6	7.8	10.1	1.7	0.047	51.8	0.6
		After coagulation	ND	7.7	15.5	1.2	0.021	52.0	
		After MF	ND	7.9	0.13	1.3	0.021	51.4	
	Mar. 2021 (16th)	Raw water	1.9	7.5	70.0	1.8	0.053	34.0	0.6
		After coagulation	ND	7.4	75.1	1.4	0.027	33.2	
		After MF	ND	7.6	0.08	1.4	0.021	34.6	

[a] Not determined.

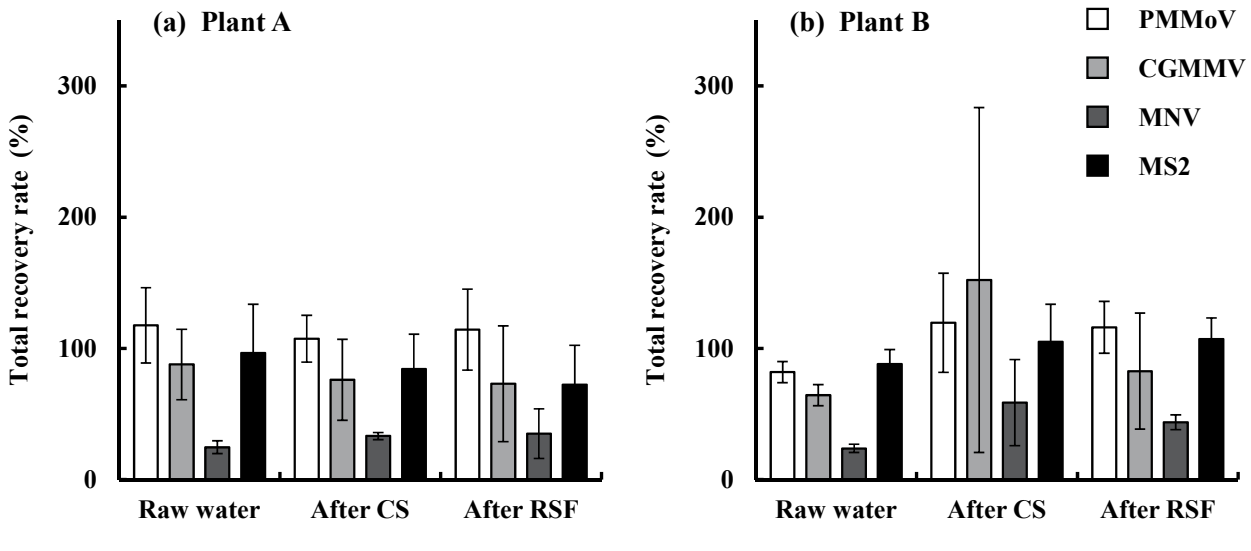
(a) Plant A
(b) Plant B
PMMoV
CGMMV
MNV
MS2
Total recovery rate (%)
300
200
100
0
Raw water
After CS
After RSF

38

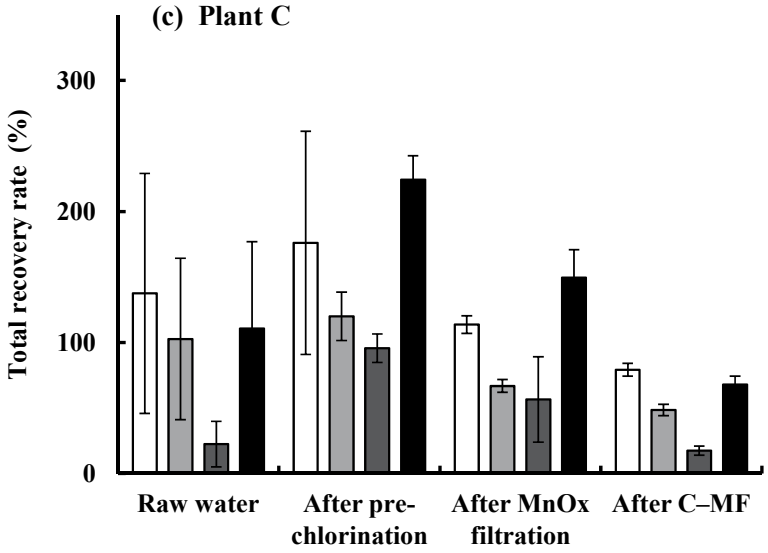
(c) Plant C
Total recovery rate (%)
300
200
100
0
Raw water
After pre-chlorination
After MnOx filtration
After C–MF

39

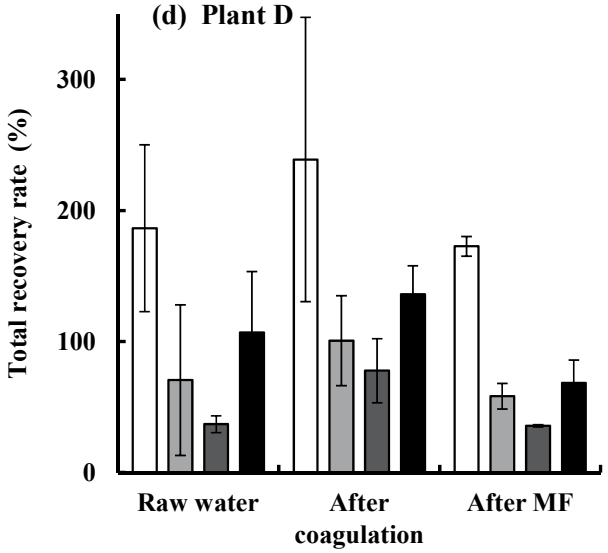
(d) Plant D
Total recovery rate (%)
300
200
100
0
Raw water
After coagulation
After MF

40

41

Fig. S1 – Total recovery rates of PMMoV and process control viruses from spiked raw and treated water samples collected at Plants A–D. Water samples collected at Plant A in November 2017, July 2018, and February 2019 (a); Plant B in August 2018 and February 2019 (b); Plant C in July 2018 and January 2019 (c); and Plant D in July 2020 and January 2021 (d) were spiked with PMMoV, CGMMV, MNV, and MS2 at initial concentrations of $10^{7–8}$ copies/mL for PMMoV and MS2, $10^{5–6}$ copies/mL for CGMMV, and $10^{6–7}$ copies/mL for MNV. Values are means and error bars indicate standard deviations (n = 2 or 3).

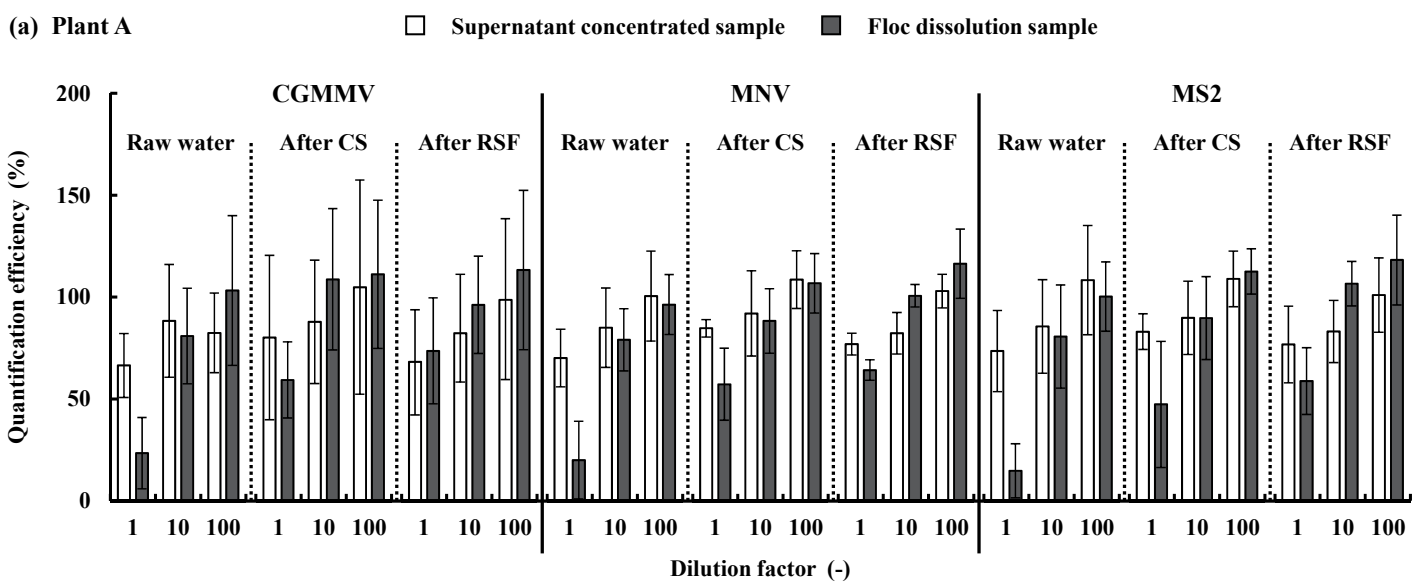
(a) Plant A
Supernatant concentrated sample
Floc dissolution sample
CGMMV
MNV
MS2
Raw water
After CS
After RSF
Quantification efficiency (%)
200
150
100
50
0
1
10
100
Dilution factor (-)

51

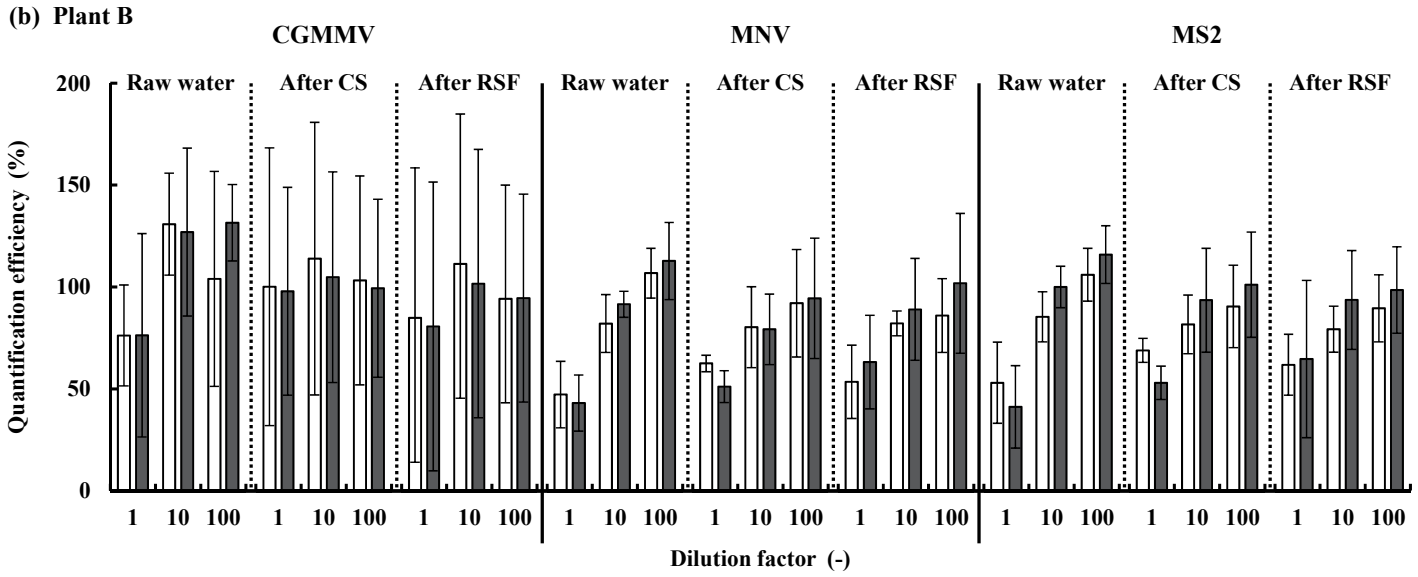
(b) Plant B
CGMMV
MNV
MS2
Raw water
After CS
After RSF
Quantification efficiency (%)
200
150
100
50
0
1
10
100
Dilution factor (-)

52

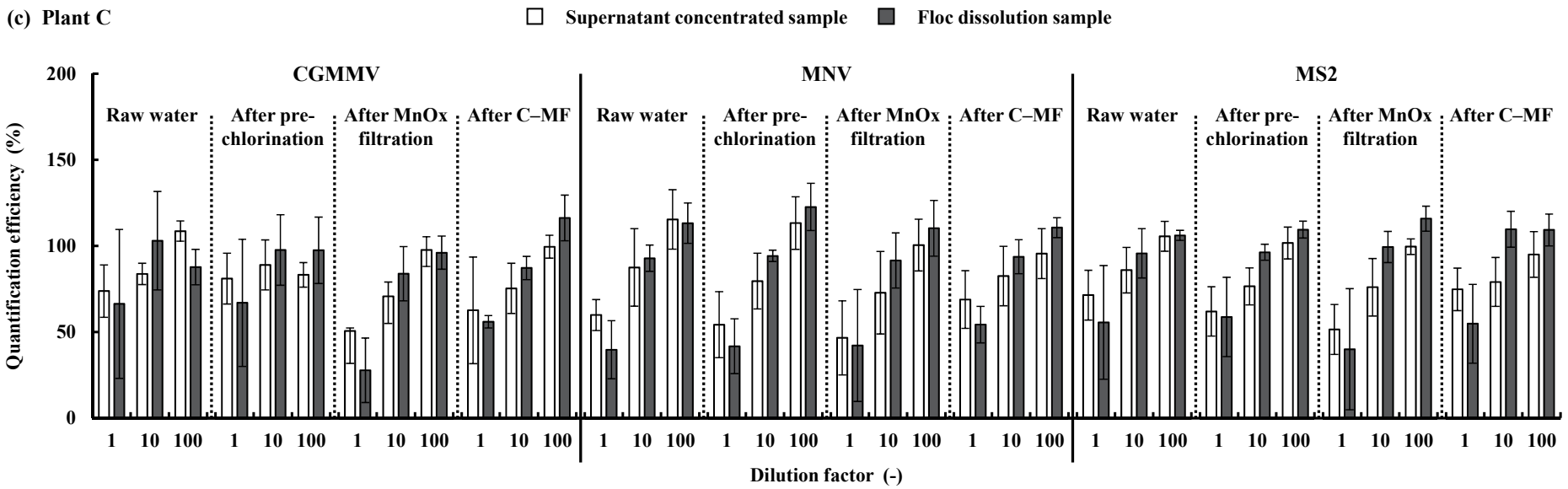
(c) Plant C
Supernatant concentrated sample
Floc dissolution sample
CGMMV
MNV
MS2
Raw water
After pre-chlorination
After MnOx filtration
After C–MF
Quantification efficiency (%)
200
150
100
50
0
1 10 100
Dilution factor (-)

53

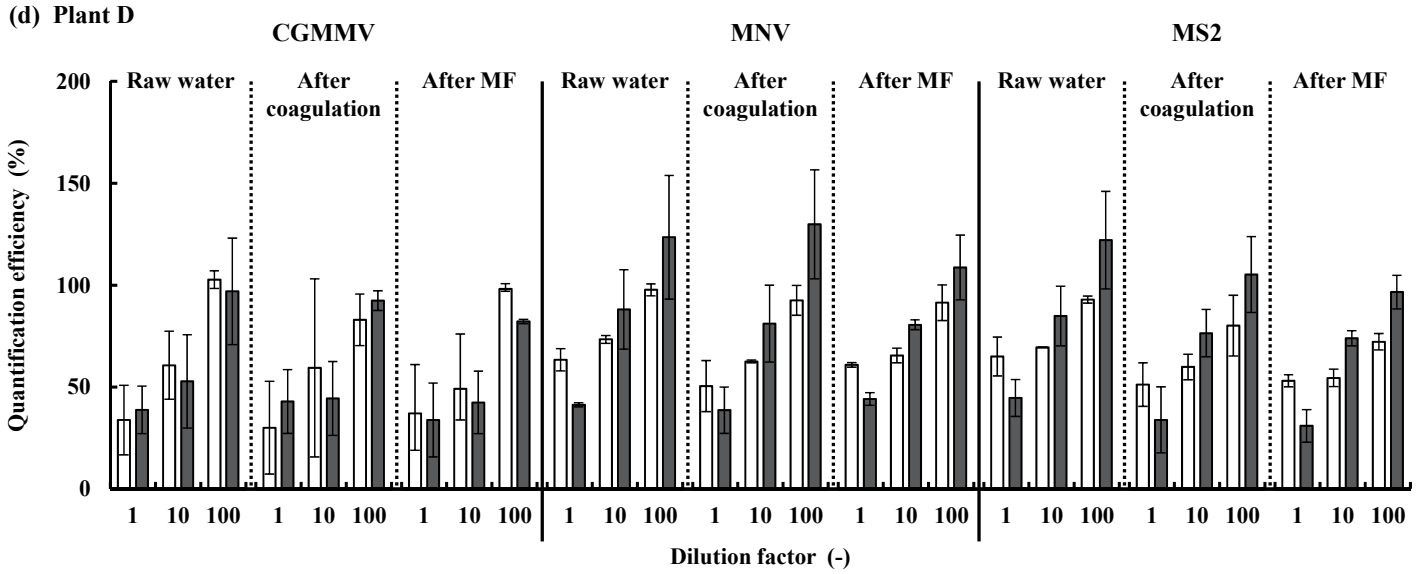
(d) Plant D
CGMMV
MNV
MS2
Raw water
After coagulation
After MF
Quantification efficiency (%)
200
150
100
50
0
1 10 100
Dilution factor (-)

54

Fig. S2 – Quantification efficiencies of process control viruses in spiked on-site concentrated samples collected at Plants A–D. Samples collected at Plant A in November 2017, December 2017, July 2018, and February 2019 (a); Plant B in November 2017, August 2018, and February 2019 (b); Plant C in July 2018, January 2019, and July 2019 (c); and Plant D in July 2020 and January 2021 (d) were spiked with CGMMV, MNV, and MS2 at initial concentrations of 10^6 copies/mL. Values are means and error bars indicate standard deviations (n = 2–4). Samples of raw water and treated water after coagulation (4 or 20 L) collected at Plant D in July 2020 were concentrated in our laboratory, not on-site.

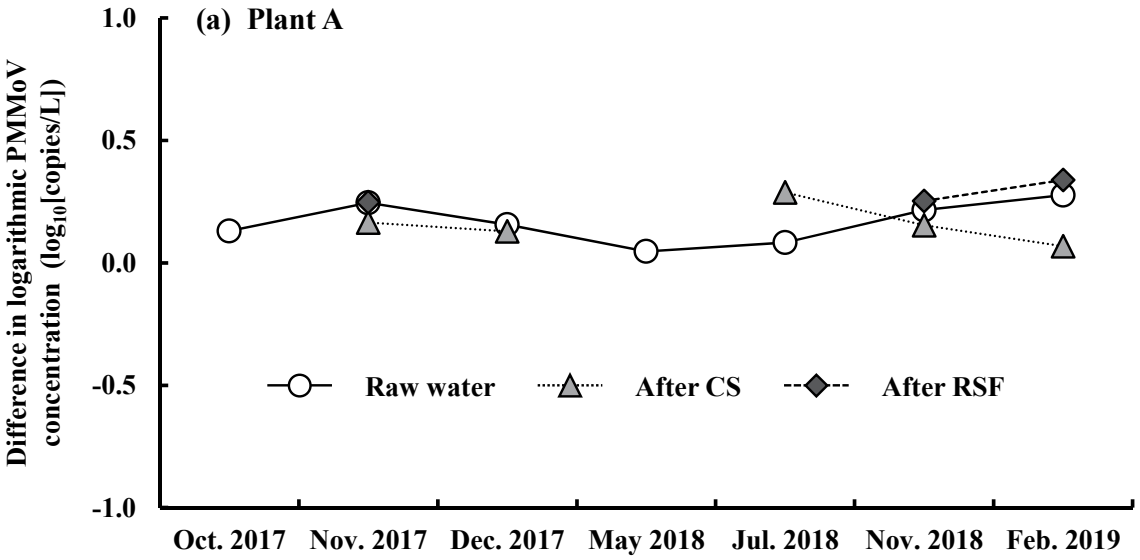
(a) Plant A
Difference in logarithmic PMMoV concentration (log_{10}[copies/L])
1.0
0.5
0.0
-0.5
-1.0
Raw water
After CS
After RSF
Oct. 2017
Nov. 2017
Dec. 2017
May 2018
Jul. 2018
Nov. 2018
Feb. 2019

63

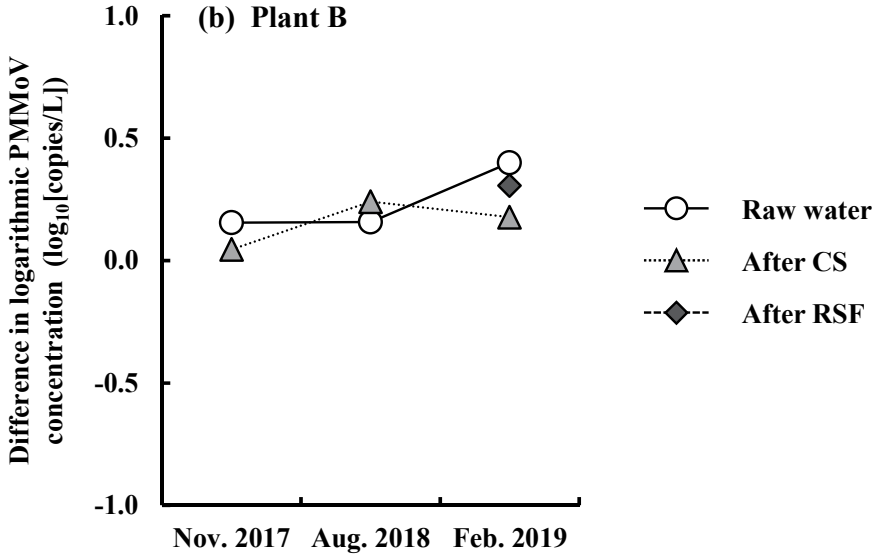
(b) Plant B
Difference in logarithmic PMMoV concentration (log_{10}[copies/L])
1.0
0.5
0.0
-0.5
-1.0
Raw water
After CS
After RSF
Nov. 2017
Aug. 2018
Feb. 2019

64

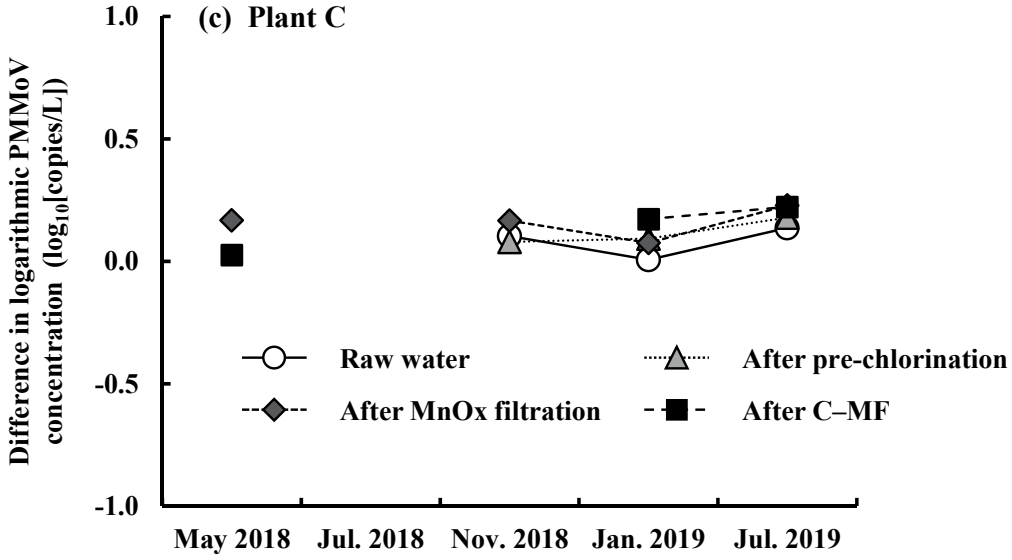
(c) Plant C
Difference in logarithmic PMMoV concentration (log_{10}[copies/L])
1.0
0.5
0.0
-0.5
-1.0
Raw water
After pre-chlorination
After MnOx filtration
After C–MF
May 2018
Jul. 2018
Nov. 2018
Jan. 2019
Jul. 2019

65

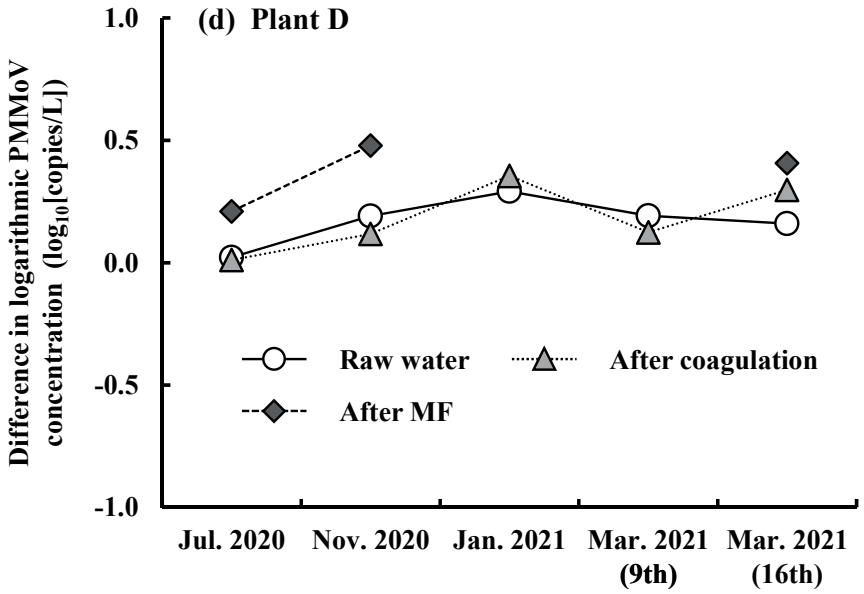

66

67

68 **Fig. S3 – Difference in concentrations of indigenous PMMoV quantified in undiluted and 10-**
69 **fold-diluted samples of raw and treated water collected at Plants A–D.** Differences were
70 calculated only when the virus concentrations could be quantified both with and without dilution.
71 Samples of raw water and treated water after coagulation (4 or 20 L) collected at Plant D in July 2020
72 were concentrated in our laboratory, not on-site.

73

74

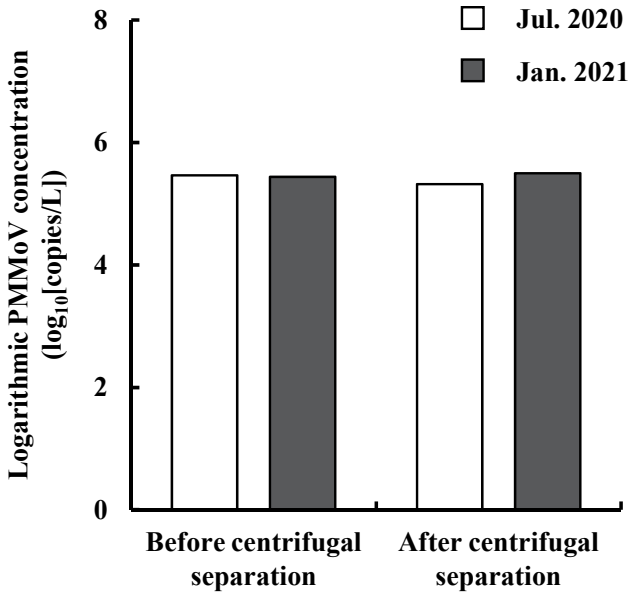

Fig. S4 – Concentrations of indigenous PMMoV in liquid phase of coagulated water samples containing powdered activated carbon before and after centrifugal separation of powdered activated carbon. Treated water samples after coagulation collected at Plant D in July 2020 and January 2021 were used.

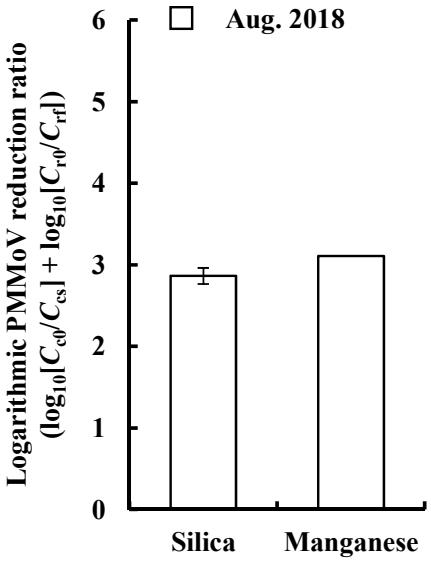

83

84

85 **Fig. S5 – Effect of sand type on reduction ratios of PMMoV in lab-scale CS–RSF.** Raw water
86 sample collected at Plant B in August 2018 was spiked with PMMoV at an initial concentration of
87 10^8 copies/mL, and then used as experimental raw water. Coagulant, PACl-1.5s (1.08 mg-Al/L). Value
88 was determined from a single experiment, or is a mean of duplicate experiments; the error bar
89 indicates standard deviation.

90

91

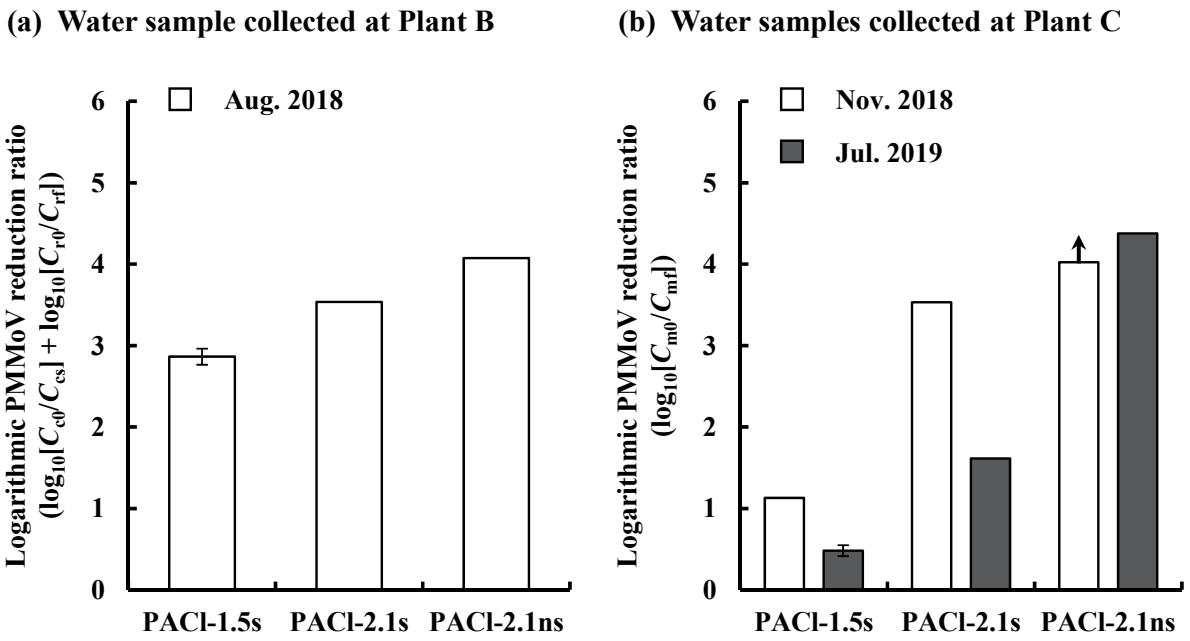

Fig. S6 – Effect of coagulant type on reduction ratios of PMMoV in lab-scale CS–RSF (a) and C–MF (b). Raw water sample collected at Plant B in August 2018 (a), and treated water samples after MnOx-coated media filtration collected at Plant C in November 2018 and July 2019 (b) were spiked with PMMoV at an initial concentration of $10^{7–8}$ copies/mL, and then used as experimental raw water. Coagulant dosage, 1.08 (a) or 0.27 (b) mg-Al/L. Silica sand was used. Values were determined from a single experiment, or are the means of duplicate experiments; the error bars indicate standard deviations. Arrow indicates that the virus concentrations were below the limit of quantification of the real-time RT-PCR.

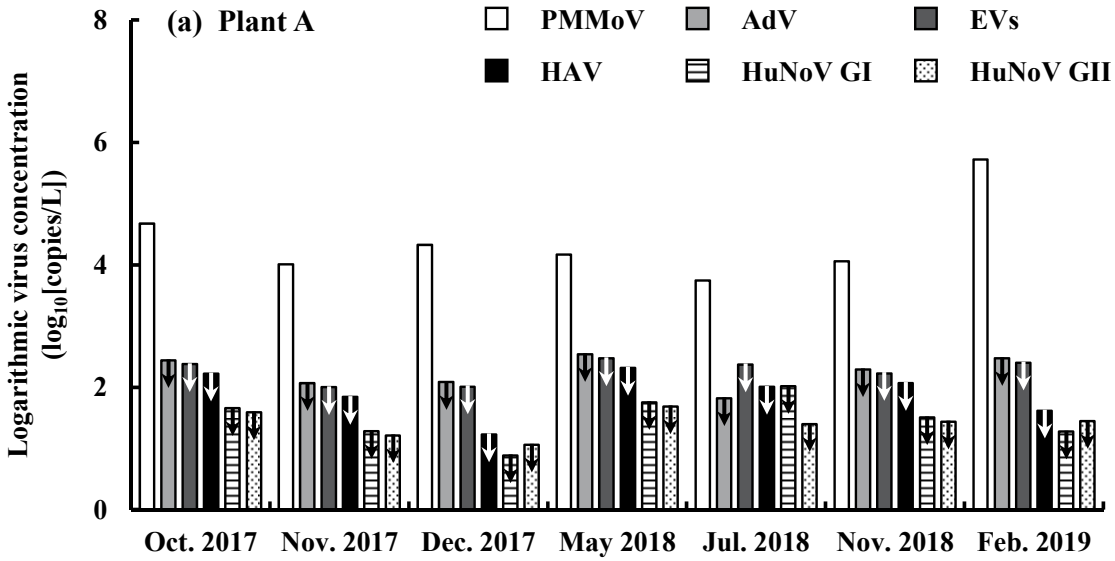
(a) Plant A
PMMoV
AdV
EVs
HAV
HuNoV GI
HuNoV GII
Logarithmic virus concentration
(log10[copies/L])
8
6
4
2
0
Oct. 2017
Nov. 2017
Dec. 2017
May 2018
Jul. 2018
Nov. 2018
Feb. 2019

104

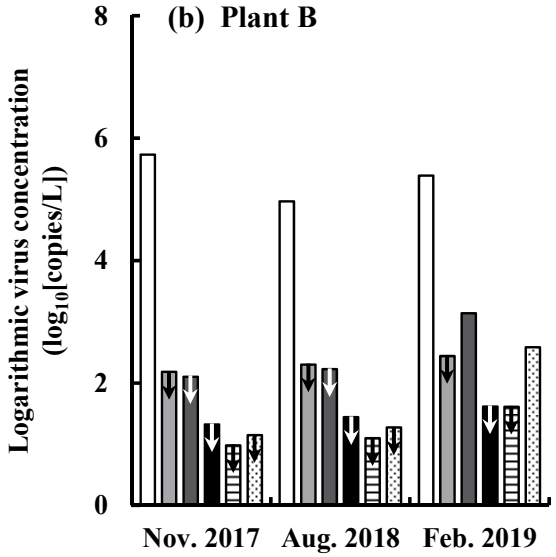
(b) Plant B
Logarithmic virus concentration
(log10[copies/L])
8
6
4
2
0
Nov. 2017
Aug. 2018
Feb. 2019

105

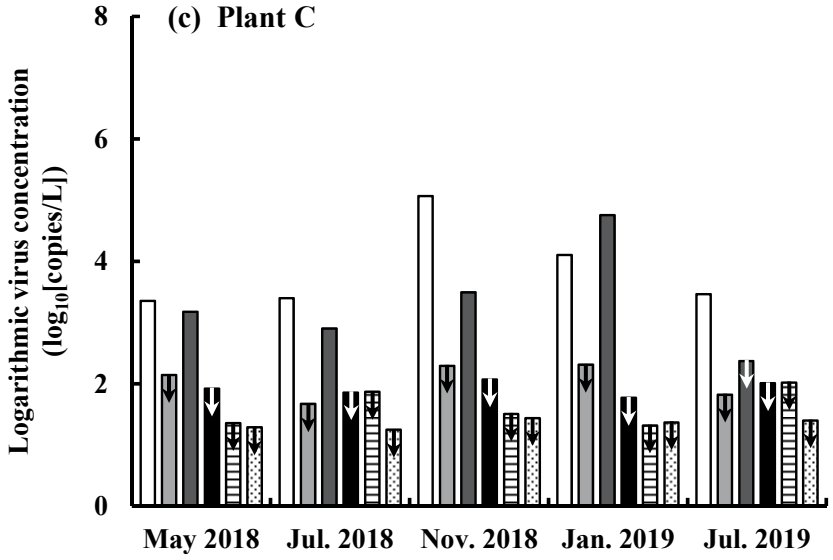
(c) Plant C
Logarithmic virus concentration
(log10[copies/L])
8
6
4
2
0
May 2018
Jul. 2018
Nov. 2018
Jan. 2019
Jul. 2019

106

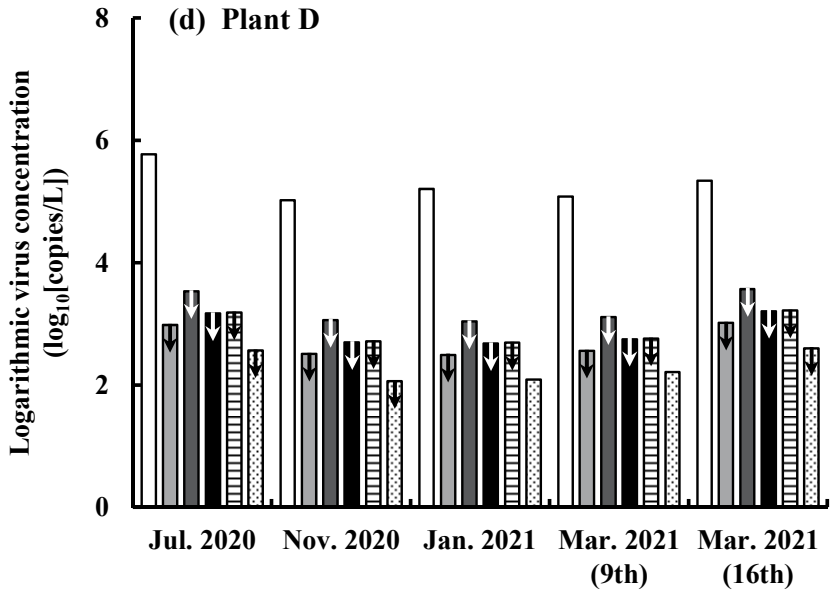

Fig. S7 – Occurrence of indigenous PMMoV and human enteric viruses in raw water at Plants A (a), B (b), C (c), and D (d). Arrows indicate that the virus concentrations were below the limit of quantification of the real-time PCR or real-time RT-PCR. Sample of raw water collected at Plant D in July 2020 (4 or 20 L) was concentrated in our laboratory, not on-site.

115 **S1. Materials and methods**

116

117 *S1.1. Virus quantification by real-time PCR or real-time RT-PCR*

118

119 Viral DNA or RNA was extracted from 200 μL of sample with a QIAamp MinElute Virus Spin Kit
120 (Qiagen, Tokyo, Japan) to obtain a final volume of DNA or RNA of 20 or 50 μL. Because the
121 concentrations of indigenous PMMoV in the on-site concentrated samples of treated water after
122 manganese oxide (MnOx)-coated media filtration and C–MF collected at Plant C in May 2018 were
123 below the quantification limit of the PCR assay when viral RNA of PMMoV was extracted from 200
124 μL of these samples to 20 μL with the above kit, viral RNA of PMMoV was extracted from 5 mL of
125 these samples to 50 μL with a QIAamp Circulating Nucleic Acid Kit (Qiagen); the quantification
126 limit was theoretically improved 10-fold compared with the QIAamp MinElute Virus Spin Kit.
127 Extracted RNA was reverse-transcribed with a High-Capacity cDNA Reverse Transcription Kit with
128 RNase Inhibitor (Applied Biosystems Japan, Tokyo, Japan); the reaction was conducted at 25 °C for
129 10 min, 37 °C for 120 min, and 85 °C for 5 s with subsequent cooling to 4 °C in a thermal cycler
130 (Thermal Cycler Dice Model TP600; Takara Bio Inc., Otsu, Japan). Extracted DNA or cDNA was
131 then amplified with TaqMan Universal Master Mix II, no UNG (Applied Biosystems Japan) with 400
132 nM primers (HQ-SEQ grade, Takara Bio Inc.), 250 nM TaqMan or TaqMan MGB probe (Applied
133 Biosystems Japan), and DNase/RNase-free distilled water. The nucleotide sequences of the primers
134 and probes are shown in Table S1. Amplification was conducted at 50 °C for 2 min, 95 °C for 10 min,
135 and then 50 cycles of 95 °C for 15 s and 60 °C for 1 min in an Applied Biosystems 7300 Real-Time
136 PCR System (Applied Biosystems Japan). A standard curve for the real-time PCR method was based
137 on the relationship between the quantification cycle (C_q value) and the copy concentration of genomic
138 DNA of AdV type 40 (ATCC VR-931D, ATCC), synthetic RNA of HuNoVs (ATCC VR-3234SD for
139 HuNoV GI, ATCC VR-3235SD for HuNoV GII, ATCC), or synthetic cDNA fragments (590 bp,

140 GeneArt Strings DNA Fragments; Thermo Fisher Scientific Inc., Waltham, MA, USA) containing the
141 PCR target sequence for PMMoV, CGMMV, EVs including CV, HAV, MNV, or MS2.
142
143 *S1.2. Characteristics and sampling points of DWTPs*
144
145 Plant A uses river water as raw water, with a treatment capacity of 5–10 × 10^5 m^3/day. Treatment
146 consists of CS and RSF. Polyaluminum chloride (PACl) with basicity ($[OH^-]/[Al^{3+}]$) 1.5 (PACl-1.5s)
147 is used as a coagulant with a dosage of 1.2–1.9 mg-Al/L on sampling days. Intermediate- and post-
148 chlorination are applied before and after RSF, respectively, throughout the year. From October 2017
149 to February 2019, samples of raw water and treated water after CS and after RSF were collected seven
150 times. In on-site sampling, filtration volumes through the NanoCeram filter were as follows: raw
151 water, 80–250 L; treated water after CS, 100–550 L; and treated water after RSF, 100–1000 L.
152 Plant B uses river water as raw water, with a treatment capacity of 1–2 × 10^6 m^3/day. Treatment
153 consists of CS, primary RSF, ozonation, biological activated carbon treatment, and secondary RSF.
154 PACl-1.5s is used as a coagulant with a dosage of 0.9–1.2 mg-Al/L on sampling days. Pre-chlorination
155 is usually applied before CS from December or January to April, and also from May to November or
156 December in case of rapid increases in ammonium ion concentrations in raw water. Intermediate- and
157 post-chlorination is applied before and after secondary RSF, respectively, throughout the year. From
158 November 2017 to February 2019, samples of raw water and treated water after CS and after primary
159 RSF were collected three times. In on-site sampling, filtration volumes through the NanoCeram filter
160 were as follows: raw water, 40–230 L; treated water after CS, 150–450 L; and treated water after
161 primary RSF, 500–1000 L.
162 Plant C uses subsoil water as raw water, with a treatment capacity of 5–10 × 10^3 m^3/day. Treatment
163 consists of MnOx-coated media filtration and C–MF. PACl-1.5s is used as a coagulant with a dosage
164 of 0.3–0.4 mg-Al/L on sampling days. Throughout the year, pre- and intermediate-chlorination is

applied before MnOx-coated media filtration, and post-chlorination is applied after C–MF. In a membrane filtration process, a hollow-fiber MF membrane module (nominal pore size, 0.1 μm; polyvinylidene difluoride) is installed. From May 2018 to July 2019, samples from raw water and treated water after pre-chlorination, MnOx-coated media filtration, and C–MF were collected five times. In on-site sampling, filtration volumes through the NanoCeram filter were as follows: raw water and treated water after pre-chlorination, 100–200 L; after MnOx-coated media filtration, 100–400 L; and after C–MF, 100–2000 L. In July 2018, 2000 L of treated water after C–MF was filtered through NanoCeram filters in duplicate, and then each filter was separately subjected to virus elution followed by organic flocculation as described in Section 2.3. The supernatant of the floc mixture from each filter (2 L each) were combined, and 4 L was concentrated to 20 mL by TF-UF. On the other hand, the flocs from each filter were dissolved in 10 mL, instead of 20 mL, of 0.15 M sodium phosphate buffer (pH 9.0), and floc dissolution samples were combined to a final volume of 20 mL. Thus, 4000 L of treated water after C–MF was concentrated to 20 mL each of the supernatant concentrated sample and the floc dissolution sample.

Plant D uses river water as raw water, with a treatment capacity of 5–10 × 10^3 m^3/day. Treatment consists of C–MF and MnOx-coated media filtration. PACl with basicity 2.1 (PACl-2.1s) is used as a coagulant with a dosage of 0.4–0.6 mg-Al/L on sampling days. Pre-, intermediate-, and post-chlorination is applied before C–MF, and before and after MnOx-coated media filtration, respectively, throughout the year. Powdered activated carbon is injected into water after pre-chlorination. In a membrane filtration process, a submerged MF membrane module (nominal pore size, 0.1 μm; ceramic) is installed. From July 2020 to March 2021, samples of raw water and treated water after coagulation and after MF were collected five times. In on-site sampling, filtration volumes through the NanoCeram filter were as follows: raw water, 4–80 L; treated water after coagulation, 4–30 L; and treated water after MF, 100–1000 L.

The water quality data for all the samples collected at the four DWTPs are shown in Table S2.

190

191 *S1.3. Evaluation of total recovery rate of viruses from spiked water samples collected at full-scale*
192 *DWTPs*

193

194 We further investigated the efficacy of the developed virus concentration method in concentrating
195 and recovering viruses from raw and treated water in full-scale DWTPs in addition to dechlorinated
196 tap water described in Section S1.2, because water quality can affect virus recovery efficiency during
197 virus concentration processes (Haramoto et al., 2018). On-site virus-spiking experiments at full-scale
198 DWTPs are ideal for directly evaluating virus recovery efficiency during on-site virus concentration
199 processes; however, such experiments are generally impossible due to compliance with biohazard
200 policies (Haramoto et al., 2018). Thus, raw and treated water samples (40 L for Plants A and C, 20 L
201 for Plant B, 10 or 20 L for Plant D) were spiked with viruses, and then concentrated in our laboratory
202 by using the developed method to evaluate the total recovery rates of viruses from spiked water
203 samples. The water samples were spiked simultaneously with the stock solutions of PMMoV and
204 CGMMV, and the purified solutions of MNV and MS2 at initial concentrations of approximately $10^{7–}$
205 ^{8} copies/mL for PMMoV and MS2, $10^{5–6}$ copies/mL for CGMMV, and $10^{6–7}$ copies/mL for MNV.
206 Spiked water was then processed with the developed method for virus concentration as described in
207 Section 2.3. To completely mitigate inhibition of the PCR assay, all concentrated samples were diluted
208 100-fold with distilled water before the PCR assay, and virus concentrations were back-calculated to
209 account for 100-fold dilution. The total virus recovery rates were calculated by using Equation 1.
210 Because filtration volumes in these experiments (10–40 L) were usually much smaller than those in
211 on-site filtration (4–2000 L), except in the case where 4–20 L of raw water or treated water after
212 coagulation were filtered on-site at Plant D, the total virus recovery rates were not used to back-
213 calculate the virus concentrations quantified in on-site concentrated samples.

214

$$R_t = (N_{cs} + N_{cf}) / N_0 \times 100\% \quad (1)$$

R_t: total virus recovery rate from spiked water (%)

N_{cs}: number of viruses in supernatant concentrated sample (copies)

N_{cf}: number of viruses in floc dissolution sample (copies)

S1.4. Evaluation of quantification efficiency of viruses in spiked on-site concentrated samples

The samples (200 μL each; undiluted or diluted 10- or 100-fold with sterilized DNase/RNase-free distilled water) were spiked simultaneously with the stock solution of CGMMV, and the purified solutions of MNV and MS2 at final concentrations of approximately 10^6 copies/mL. In addition, sterilized DNase/RNase-free distilled water (200 μL) was spiked with the solutions of the three viruses, and defined as a control sample without any inhibition of the PCR assay. The spiked samples were subjected to RNA extraction, RT, and real-time PCR. The quantification efficiency was determined according to Equation 2, and used only to evaluate the extent of inhibition of the PCR assay.

$$E_q = N_q / N_{q0} \times 100\% \quad (2)$$

E_q: quantification efficiency (%)

N_q: number of viruses in concentrated sample (copies)

N_{q0}: number of viruses in control sample (copies)

S1.5. Coagulants

To mimic full-scale CS–RSF (Plants A and B) and C–MF (Plant C), we used the same sulfated PACl products with basicity 1.5 (PACl-1.5s) as used at the three DWTPs (North PACl, 2.4% sulfate

240 [w/w], Hokkaido Soda Co., Tomakomai, Japan; Tai PACl, 2.8% sulfate [w/w], Taimei Chemicals Co.,
241 Minamiminowa, Japan). To discuss the effect of coagulant type on virus reduction in full-scale CS–
242 RSF and C–MF, we used sulfated high-basicity PACl with basicity 2.1 (PACl-2.1s; PACl 700A,
243 2.2%–2.9% sulfate [w/w], Taki Chemical Co., Kakogawa, Japan); and non-sulfated, high-basicity
244 PACl with basicity 2.1 (PACl-2.1ns; not commercially available, kindly supplied by Taki Chemical
245 Co.). Immediately prior to use, the coagulants were diluted with Milli-Q water (Milli-Q Advantage;
246 Millipore Corp.).
247
248 *S1.6. Lab-scale virus-spiking CS–RSF experiments*
249
250 Batch virus-spiking CS experiments were conducted with raw water samples collected at Plant A
251 (4 L) and Plant B (2 L) in square plastic beakers at 20 °C. The samples were spiked with the stock
252 solution of PMMoV at an initial concentration of approximately 10^8 copies/mL. As a result of spiking,
253 <0.1 mg/L of dissolved organic carbon was unintentionally introduced. After enough HCl or NaOH
254 was added to bring the final pH to 7.0, a coagulant was injected at 0.54, 1.08, 1.62, or 2.16 mg-Al/L.
255 Coagulant dosages were determined by considering those applied at Plant A (1.2–1.9 mg-Al/L) and
256 Plant B (0.9–1.2 mg-Al/L) on the sampling days. The water was stirred rapidly with an impeller stirrer
257 for 1 min ($G = 200\ s^{-1}$, 120 rpm for 4 L, 197 rpm for 2 L), then slowly for 10 min ($G = 20\ s^{-1}$, 26 rpm
258 for 4 L, 42 rpm for 2 L), and then was allowed to stand without stirring for 60 min to settle the
259 generated aluminum floc particles. Samples were taken from the beaker for quantification of the virus
260 concentrations (before coagulation, C_{c0}; after settling, C_{cs}), and quantified by the PCR assay without
261 the virus concentration processes.
262 After the batch CS experiments, RSF experiments were conducted with a plastic column (diameter,
263 3.6 cm; length, 100 cm) packed with silica sand or manganese sand at 20 °C. Silica sand was washed
264 with Milli-Q water, and dried at 105 °C for 6 h. To wash manganese sand, tap water supplied by Plant

A was filtered through a polytetrafluoroethylene membrane filter (nominal pore size, 0.20 μm; Toyo Roshi Kaisha), and then sodium hypochlorite (NaClO; Fujifilm Wako Pure Chemical Corp., Osaka, Japan) was added to obtain a free-chlorine concentration of 0.7 mg-Cl_2/L. Manganese sand was then washed with filtered and chlorinated tap water, and dried at 105 °C for 6 h. The washed silica sand or manganese sand was gradually added into the column to achieve a 60-cm filter depth. Approximately 5 L of Milli-Q water (for silica sand), or filtered and chlorinated tap water (for manganese sand) was pumped upward through the column, and then another volume (approximately 5 L) of Milli-Q water (for silica sand), or filtered and chlorinated tap water (for manganese sand) was pumped downward through the column with the peristaltic pump to remove fines in the filter media. This upward-and-downward washing procedure was done twice before each experiment. Sufficient removal of fines was confirmed by the fact that the turbidity of the filter effluent after washing was <0.2 NTU. Next, approximately 3 L (when 4 L of water was used in CS experiments) or 1.5 L (when 2 L of water was used in CS experiments) of the supernatant from the settled sample was transferred from the beaker to another beaker as raw water for RSF experiments. When raw water samples collected at Plant A were used for CS experiments, NaClO was added to the supernatant from the settled sample to obtain a free-chlorine concentration of 0.7 mg-Cl_2/L, because intermediate-chlorination was applied at Plant A before RSF. Under this condition, the residual free-chlorine concentration in sand filtrates was almost the same as that in treated water after RSF at Plant A on the sampling days (approximately 0.2 mg-Cl_2/L). The supernatant from the settled sample was continuously mixed with a magnetic stirrer at 300 rpm (for 3 L of water) or 150 rpm (for 1.5 L of water) during the experiments. After mixing for 5 min, the water was fed into the column at a constant flow rate (120 m/day) with the peristaltic pump. Taking the residence time of water in the sand column into consideration, samples were taken from the beaker at three pre-determined sampling times during filtration, and from the sand filtrate after 15, 20, and 25 min (for 3 L of water), or 16.5, 18, and 19.5 min (for 1.5 L of water) of filtration for quantification of virus concentrations (raw water for RSF, C_{r0}; sand filtrate, C_{rf}), and quantified

by the PCR assay without the virus concentration processes. The reduction ratios of PMMoV were expressed as the averages of the three time points for each volume of water, because the reduction ratios were almost independent of filtration time (data not shown). Washed filter medium not yet used in any experiment was used in each experiment to avoid viral and particle cross-contamination.

S1.7. Lab-scale virus-spiking C–MF experiments

Experiments were conducted with samples (500 mL) of treated water after MnOx-coated media filtration (i.e., water just before C−MF) collected at Plant C in square plastic beakers at 20 °C. The lab-scale MF membrane was rinsed by filtering approximately 500 mL of Milli-Q water, and sterilized for 60 min by circulating a solution containing 2000 mg-Cl_2/L of free chlorine; the rinsing step was repeated prior to use to remove any residual free chlorine. NaClO was added to the samples and mixed for 1 min to obtain a free-chlorine concentration of 0.6 mg-Cl_2/L, similar to that in treated water after MnOx-coated media filtration at Plant C on the sampling days. The samples were then spiked with the stock solution of PMMoV at an initial concentration of approximately $10^{7–8}$ copies/mL. As a result of spiking, <0.1 mg/L of dissolved organic carbon was unintentionally introduced. After enough HCl or NaOH was added to bring the final pH to 7.0, a coagulant was injected at 0.27, 0.54, or 1.08 mg-Al/L. Coagulant dosages were determined by considering those applied at Plant C on the sampling days (0.3–0.4 mg-Al/L). The water was stirred rapidly (G = 200 s^{-1}, 97 rpm) with the impeller stirrer during the experiments. After stirring for 1 min, water filtration through the membrane was started at a constant flow rate (1 m/day) with the peristaltic pump, with a cross-flow volume twice the filtration volume. Taking the residence time of water in the membrane module into consideration, samples were taken from the beaker before coagulation, and from the MF filtrate after 4.5, 5.5, 6.5, 7.5, and 8.5 min of filtration for quantification of virus concentrations (before coagulation, C_{m0}; MF filtrate, C_{mf}), and quantified by the PCR assay without the virus concentration processes. The reduction ratios of

PMMoV were expressed as the averages of the five time points, because the reduction ratios were almost independent of filtration time (data not shown). The membrane was re-used after the rinsing–sterilization procedure described above.

S1.8. Development of a virus concentration method

In our laboratory at Hokkaido University (Sapporo, Japan), tap water (1000 L) supplied by Plant A (CS–RSF) was dechlorinated with sodium thiosulfate at a final concentration of 5 mg/L, and was spiked with the stock solution of PMMoV at an initial concentration of approximately 10^8 copies/mL. The spiked water was filtered and concentrated as described in Section 2.3, except that supernatant concentrated samples were not filtered through the hydrophilic cellulose acetate membrane filter.

To completely mitigate inhibition of the PCR assay, all concentrated samples were diluted 100-fold with sterilized DNase/RNase-free distilled water before the PCR assay, and virus concentrations were back-calculated to account for 100-fold dilution. The total recovery rate of PMMoV from spiked water was calculated by using Equation 1. The retention rate of PMMoV on the filter and its elution rate were calculated by using Equations 3 and 4, respectively.

$$R_r = (N_0 - N_f) / N_0 \times 100\% \quad (3)$$

R_r: virus retention rate on the NanoCeram filter (%)

N_f: number of viruses in filtrate (copies)

N_0: number of viruses in spiked water (copies)

$$R_e = N_e / (N_0 - N_f) \times 100\% \quad (4)$$

R_e: virus elution rate from the NanoCeram filter using BE solution (%)

N_e: number of viruses in 2 L of eluate (copies)

340

341 *S1.9. Virus-spiking organic flocculation experiment*

342

343 The BE solution (pH 9.5; 250 mL) was spiked simultaneously with the stock solutions of PMMoV
344 and CGMMV, and the purified solutions of AdV, CV, HAV, MNV, and MS2 at initial concentrations
345 of approximately 10^{8-9} copies/mL for PMMoV, 10^{7-8} copies/mL for CGMMV, CV, and MNV, 10^{7}
346 copies/mL for AdV, 10^{6} copies/mL for HAV, and 10^{10} copies/mL for MS2. Spiked BE solution was
347 then subjected to organic flocculation as described in Section 2.3. Separated flocs were dissolved in
348 2.5 mL of 0.15 M sodium phosphate buffer (pH 9.0), and virus concentrations in floc dissolution
349 samples (2.5 mL) and in the supernatant of the floc mixture (250 mL; not concentrated by TF-UF)
350 were quantified to determine the virus recovery rate in floc dissolution samples (Equation 5) and in
351 the supernatant of the floc mixture (Equation 6).

352

353 $$R_f = N_{cf} / N_{b0} \times 100\% \quad (5)$$

354 R_f: virus recovery rate in floc dissolution sample (%)

355 N_{cf}: number of viruses in floc dissolution sample (copies)

356 N_{b0}: number of viruses in spiked BE solution (copies)

357

358 $$R_s = N_s / N_{b0} \times 100\% \quad (6)$$

359 R_s: virus recovery rate in supernatant of floc mixture (%)

360 N_s: number of viruses in supernatant of floc mixture (copies)

361

362 **S2. Results and discussion**

363

S2.1. Effects of pH of BE solution, soaking times for the third and fourth elution, and filter type on virus recovery rates

At pH 9.0, the elution rate of PMMoV with a soaking time of 15 min for the third and fourth elution (28%; Table 1, Method 1) was similar to that with a soaking time of 30 min (32%; Table 1, Method 2). At pH 9.5, the elution rate of PMMoV increased to 60% with a soaking time of 30 min (Table 1, Method 3). Thus, a soaking time of 30 min for the third and fourth elution, and pH 9.5 of BE solution were used in subsequent experiments.

The retention rates of PMMoV between two types of the NanoCeram filters (P2.5-5DP and VS2.5-5) were similar (Table 1, Methods 3 and 4), probably because of the same effective filtration area (0.129 m^2), and the elution and total recovery rates of PMMoV were also similar (Table 1, Methods 3 and 4). Because VS2.5-5 was developed specifically to concentrate viruses and pre-sterilized, we used it in subsequent experiments.

S2.2. Efficacy of the developed virus concentration method in concentrating and recovering MNV

To confirm that the developed virus concentration method can also effectively concentrate and recover viruses that are recovered mainly in floc dissolution samples, we evaluated the total recovery rates of PMMoV in addition to MNV. Dechlorinated tap water (100 L) was spiked simultaneously with PMMoV and MNV, and then filtered and concentrated. The total recovery rate was 106% for PMMoV and 30% for MNV (data not shown). Cashdollar et al. (2013) filtered (1) 1500−1900 L of non-spiked groundwater followed by 10 L of MNV-spiked groundwater, (2) 80 L of non-spiked surface water followed by 10 L of MNV-spiked surface water, and (3) 10 L of MNV-spiked reagent-grade water, and concentrated all volumes to 400 μL by using Method 1615, and reported total recovery rates of 30%, 6%, and 0.6%–8%, respectively. The total recovery rate of MNV obtained in

the present study was similar to or higher than those obtained by Cashdollar et al. (2013), indicating that the developed method can effectively concentrate and recover PMMoV along with MNV, which is recovered mainly in floc dissolution samples, from large volumes of dechlorinated tap water.

S2.3. Virus reduction by powdered activated carbon adsorption

Samples of treated water after coagulation from Plant D contained powdered activated carbon, and were directly filtered through the NanoCeram filter. Even if PMMoV was adsorbed on powdered activated carbon, it could be retained on the filter, and desorbed from powdered activated carbon during subsequent virus elution. If so, we may overestimate the concentrations of indigenous PMMoV in treated water after coagulation, and underestimate its reduction ratios by adsorption on powdered activated carbon. To investigate the possible contribution of adsorption on powdered activated carbon to the reduction of PMMoV, coagulated water samples containing powdered activated carbon were centrifuged at 4000 × *g* for 10 min to separate powdered activated carbon from the liquid phase of these samples. The concentrations of indigenous PMMoV, as quantified by the PCR assay without the virus concentration processes, in the liquid phase before and after centrifugal separation of powdered activated carbon were similar (Fig. S4), suggesting that the contribution of adsorption on powdered activated carbon to the reduction of PMMoV was negligible.

S2.4. Effect of sand type on virus reduction in CS–RSF

The PMMoV reduction ratios obtained with silica sand and manganese sand were almost the same (Fig. S5), suggesting that sand type did not affect virus reduction efficiency in CS–RSF. Thus, silica sand was used in lab-scale CS–RSF with the raw water sample collected at Plant B in August 2018, because pre-chlorination before CS was not applied on the sampling day.

S2.5. Validation of lab-scale virus-spiking CS–RSF and C–MF experiments

To validate whether lab-scale virus-spiking CS–RSF and C–MF successfully mimicked full-scale CS–RSF (Plants A and B) and C–MF (Plants C and D) in terms of virus reduction, we compared the reduction ratios of PMMoV in lab-scale CS–RSF and C–MF with those in full-scale CS–RSF and C–MF. In the raw water sample collected at Plant A in July 2018 (Fig. 4a), the reduction ratio of PMMoV in lab-scale CS–RSF at a coagulant dosage of 1.08 mg-Al/L was >1-$\log_{10}$ higher than that in full-scale CS–RSF at 1.24 mg-Al/L; the reason for this difference is unclear. In the raw water sample collected at Plant A in February 2019 (Fig. 4a), the reduction ratios of PMMoV in lab-scale CS–RSF at 1.08 or 1.62 mg-Al/L were similar to that in full-scale CS–RSF at 1.51 mg-Al/L. In the raw water sample from Plant B (Fig. 4b), the reduction ratio of PMMoV in full-scale CS–RSF at 0.98 mg-Al/L was within the range of those in lab-scale CS–RSF at 0.54–1.08 mg-Al/L. These results indicate that lab-scale CS–RSF with the samples collected at Plant A in February 2019 and Plant B in August 2018 successfully mimicked full-scale CS–RSF at Plants A and B, respectively, in terms of virus reduction, but that lab-scale CS–RSF with the sample collected at Plant A in July 2018 did not.

In treated water samples after MnOx-coated media filtration collected at Plant C in November 2018 and July 2019 (Fig. 4c), the reduction ratios of PMMoV in lab-scale C–MF at 0.27 mg-Al/L were similar to those in full-scale C–MF at 0.27 or 0.33 mg-Al/L. This result indicates that lab-scale C–MF successfully mimicked full-scale C–MF in terms of virus reduction.

S2.6. Effect of coagulant type on virus reduction in CS–RSF and C–MF

In lab-scale CS–RSF, the reduction ratio of PMMoV were increased from 2.9-$\log_{10}$ with PACl-1.5s to 3.5-$\log_{10}$ with PACl-2.1s, and reached 4.1-$\log_{10}$ with PACl-2.1ns (Fig. S6a). These results indicate

439 that coagulant type affected virus reduction efficiency in CS–RSF, and that high-basicity PACls,
440 especially the non-sulfated one, were more effective for virus reduction than PACl-1.5s. Our research
441 group has reported that colloid charge densities of PACl-2.1s and PACl-2.1ns are higher than that of
442 PACl-1.5s; PACl-2.1ns has the highest colloid charge density, probably due to the large amounts of
443 colloidal aluminum species and the absence of sulfate (Shirasaki et al., 2014). Thus, the high colloid
444 charge densities of PACl-2.1s and PACl-2.1ns, especially that of PACl-2.1ns, likely resulted in their
445 high virus reduction ratios compared with that of PACl-1.5s.
446 The turbidities of sand filtrates obtained with PACl-1.5s and PACl-2.1s were almost the same (data
447 not shown), indicating that the use of PACl-2.1s instead of PACl-1.5s in full-scale CS–RSF could
448 improve virus reduction efficiency without decreasing the ability to reduce turbidity. In contrast, the
449 turbidities of sand filtrates obtained with PACl-2.1ns were higher than those obtained with PACl-1.5s
450 (data not shown), indicating that the use of PACl-2.1ns instead of PACl-1.5s in full-scale CS–RSF is
451 not appropriate for turbidity reduction, despite its highest effectiveness for virus reduction.
452 In lab-scale C–MF, the reduction ratios of PMMoV were increased from 0.5–1.1-$\log_{10}$ to 1.6–4.4-
453 $\log_{10}$ by the use of high-basicity PACls instead of PACl-1.5s; in particular, PACl-2.1ns provided the
454 PMMoV reduction ratios of >4-$\log_{10}$ (Fig. S6b). These results indicate that coagulant type strongly
455 affected virus reduction efficiency in C–MF, and that high-basicity PACls, especially the non-sulfated
456 one, were more effective for virus reduction than PACl-1.5s.
457
458 **References**
459
460 Cashdollar, J.L., Brinkman, N.E., Griffin, S.M., McMinn, B.R., Rhodes, E.R., Varughese, E.A.,
461 Grimm, A.C., Parshionikar, S.U., Wymer, L., Fout, G.S., 2013. Development and evaluation of
462 EPA Method 1615 for detection enterovirus and norovirus in water. Appl. Environ. Microbiol. 79
463 (1), 215–223.

Haramoto, E., Kitajima, M., Kishida, N., Konno, Y., Katayama, H., Asami, M., Akiba, M., 2013. Occurrence of pepper mild mottle virus in drinking water sources in Japan. Appl. Environ. Microbiol. 79 (23), 7413–7418.

Haramoto, E., Kitajima, M., Hata, A., Torrey, J.R., Masago, Y., Sano, D., Katayama, H., 2018. A review on recent progress in the detection methods and prevalence of human enteric viruses in water. Water Res. 135, 168–186.

Hongyun, C., Wenjun, Z., Qinsheng, G., Qing, C., Shiming, L., Shuifang, Z., 2008. Real time TaqMan RT-PCR assay for the detection of Cucumber green mottle mosaic virus. J. Virol. Methods. 149 (2), 326–329.

Jothikumar, N., Cromeans, T.L., Sobsey, M.D., Robertson, B.H., 2005. Development and evaluation of a broadly reactive TaqMan assay for rapid detection of hepatitis A virus. Appl. Environ. Microbiol. 71 (6), 3359–3363.

Katayama, H., Shimasaki, A., Ohgaki, S., 2002. Development of a virus concentration method and its application to detection of enterovirus and Norwalk virus from coastal seawater. Appl. Environ. Microbiol. 68 (3), 1033–1039.

Kitajima, M., Oka, T., Takagi, H., Tohya, Y., Katayama, H., Takeda, N., Katayama, K., 2010. Development and application of a broadly reactive real-time reverse transcription-PCR assay for detection of murine noroviruses. J. Virol. Methods. 169 (2), 269–273.

Ko, G., Jothikumar, N., Hill, V.R., Sobsey, M.D., 2005. Rapid detection of infectious adenoviruses by mRNA real-time RT-PCR. J. Virol Methods. 127 (2), 148–153.

O'Connell, K.P., Bucher, J.R., Anderson, P.E., Cao, C.J., Khan, A.S., Gostomski, M.V., Valdes, J.J., 2006. Real-time fluorogenic reverse transcription-PCR assays for detection of bacteriophage MS2. Appl. Environ. Microbiol. 72 (1), 478–483.

487 Shieh, Y.S.C., Wait, D., Tai, L., Sobsey, M.D., 1995. Methods to remove inhibitors in sewage and
488 other fecal wastes for enterovirus detection by the polymerase chain-reaction. J. Virol. Methods.
489 54 (1), 51–66.
490 Shirasaki, N., Matsushita, T., Matsui, Y., Oshiba, A., Marubayashi, T., Sato, S., 2014. Improved virus
491 removal by high-basicity polyaluminum coagulants compared to commercially available
492 aluminum-based coagulants. Water Res. 48, 375–386.
493 Vega, E., Barclay, L., Gregoricus, N., Williams, K., Lee, D., Vinjé, J., 2011. Novel surveillance
494 network for norovirus gastroenteritis outbreaks, United States. Emerg. Infect. Dis. 17 (8), 1389–
495 1395.
496 Zhang, T., Breitbart, M., Lee, W.H., Run, J.Q., Wei, C.L., Soh, S.W.L., Hibberd, M.L., Liu, E.T.,
497 Rohwer, F., Ruan, Y.J., 2006. RNA viral community in human feces: prevalence of plant pathogenic
498 viruses. PLoS Biol. 4 (1), 108–118.
499